Self-Supporting Oxygen Reduction Electrocatalysts Made from a Nitrogen-Rich Network Polymer

Yong Zhao,[†] Kazuya Watanabe,*,[†,‡] and Kazuhito Hashimoto*,[†,§]

[†]ERATO/JST, HASHIMOTO Light Energy Conversion Project, The University of Tokyo, 4-6-1 Komaba, Meguro-ku, Tokyo 153-8505, Japan

[‡]Tokyo University of Pharmacy and Life Sciences, 1432-1 Horinouchi, Hachioji, Tokyo 192-0392, Japan

[§]Department of Applied Chemistry, The University of Tokyo, 7-3-1 Hongo, Bunkyo-ku, Tokyo 113-8656, Japan

Ⓢ *Supporting Information*

ABSTRACT: We report the design, synthesis, and evaluation of a new type of non-precious-metal catalyst made from network polymers. 2,6-Diaminopyridine was selected as a building-block monomer for the formation of a nitrogen-rich network polymer that forms self-supporting spherical backbone structures and contains a high density of metal-coordination sites. A Co-/Fe-coordinating pyrolyzed polymer exhibited a high specific oxygen reduction activity with onset and half-wave potentials of 0.87 and 0.76 V vs RHE, respectively, in neutral media. There was no crossover effect of organics on its activity. The power output of a microbial fuel cell equipped with this catalyst on its cathode was more than double the output with a commercial 20 wt % Pt/C catalyst.

Oxygen reduction reaction (ORR) catalysts are essential for clean energy technologies such as metal−air batteries[1] and fuel cells.[2] Currently, the prohibitive cost and scarcity of the precious metals used for ORR catalysts limit the large-scale commercialization of these technologies.[3] Extensive efforts have been directed to the development of non-precious-metal catalysts (NPMCs) that facilitate the ORR on electrodes.[2b,4] One of the most promising NPMCs for the ORR is transition-metal-coordinating C/N materials. Studies of these catalysts were initiated after the discovery of the ORR activity of cobalt phthalocyanine,[5] followed by the investigation of its analogues (metal/N-containing macrocycles) to improve their catalytic activities.[6] To avoid the use of expensive macrocycles, attempts have also been made to develop other types of NPMCs, including N-containing graphitic structures[7] and metal-coordinating polymers.[8] Among them, pyrolyzed metal-coordinating polymers are considered to be very attractive candidates for NPMCs at various pH. To date, these efforts have utilized N-containing polymers such as polyacrylonitrile,[8a] polypyrrole,[8b] *p*-toluene-sulfonic acid-doped polypyrrole,[8c] and polyaniline (PANI),[8d] and catalysts have been constructed by doping carbon supports with these polymers (polymer/C). The highest ORR activity has been reported for a Co-/Fe-coordinating PANI/C (CoFe-PANI/C) catalyst, whose activity at a catalyst loading of 0.6 mg cm^{-2} was equivalent to that of a 20 wt % Pt/C catalyst loaded at 0.02 mg$_{Pt}$ cm^{-2} in electrochemical tests.[8d] The activity of that catalyst was also shown to be stable for at least 700 h in fuel-cell tests.[8d] Although the reaction mechanisms are still not fully

understood, these studies have suggested factors that should be considered for synthesizing active NPMCs, including polymer structure, type of nitrogen, transition-metal species, pyrolysis temperature, and carbon-support morphology.[2b,8d]

The present study was conducted to develop active and stable NPMCs that are suitable for use as cathode catalysts in green-energy devices, including microbial fuel cells (MFCs). Recently, extensive research has been performed on MFCs that will be applied to the conversion of biomass into electricity and the treatment of wastewaters, whereas the lack of cheap and organics-resistant ORR catalysts hampers their large-scale application.[2a,c,3b] Researchers have attempted to use some NPMCs as ORR catalysts in MFCs, but the ORR activity still needs to be improved in terms of the onset and half-wave potentials.[2a,9] Here we examined N-rich multidimensional network polymers that contain a high density of intramolecular metal (e.g., Co, Fe) coordination sites. Different from the liner polymers previously used for NPMCs,[8] some network polymers are known to self-organize spherical backbone structures [e.g., poly(divinylbenzene)[10]] that can be used as self-supporting catalysts. Furthermore, we considered that with conductive polymers as precursors, electrically conductive electrode catalysts could be synthesized at relatively low pyrolysis temperatures, which could reduce the loss of nitrogen during pyrolysis. On the basis of these ideas, we selected 2,6-diaminopyridine (DAP) as a building-block monomer for the formation of a network polymer that forms self-supporting spherical backbone structures (∼500 nm in diameter) and contains a high density of metal-coordination sites. We found that a Co- and Fe-coordinating pyrolyzed polymer treated with NH$_3$ exhibits a high specific ORR activity close to that of a 20 wt % Pt/C (hereafter "Pt/C") catalyst. We also found that the ORR activity of metal-coordinating poly(DAP) (M-PDAP) in electrochemical tests is durable and has no crossover effects of organics.

To synthesize N-containing network polymers, several monomer candidates were examined, such as DAP, amino-pyridine, and aminopyrazine. They were polymerized in the presence of an oxidizer (ammonium peroxydisulfate) and evaluated in terms of their abilities to form stable polymers and macrostructures as well as their N contents. The synthetic procedures are outlined in Figure 1 and described in detail in the
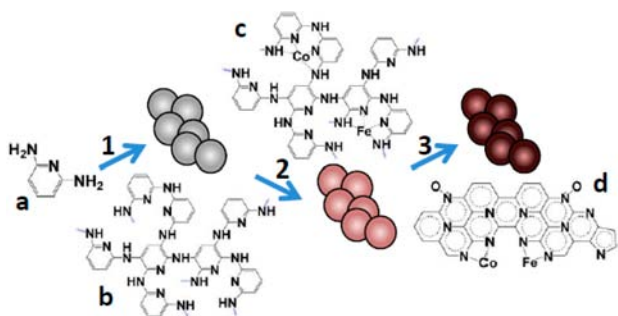
Figure 1. Synthesis of pyrolyzed M-PDAP. Steps: (1) polymerization and spontaneous sphere formation; (2) metal coordination; (3) pyrolysis at 700 °C in the presence of NH_3. Structures: (a) DAP; (b) PDAP; (c) M-PDAP; (d) M-PDAP after pyrolysis and NH_3 treatment.

Supporting Information (SI). The best results were obtained with DAP, which can easily be polymerized, spontaneously forming stable and uniform spherical structures (~0.5 μm in diameter) and containing a high percentage of N (40 wt % before pyrolysis). After coordination of transition metals (Co and/or Fe) to PDAP, it was pyrolyzed to form metal-coordinating graphitic structures (Figure 1). We examined the pyrolysis temperature (600−900 °C), since previous studies showed that the temperature greatly influences the ORR activities of NPMCs.[15] Electrochemical tests showed that the best electrode catalyst was obtained by pyrolyzing Co-PDAP at 700 °C (Figure S1 and Table S1 in the SI). Also, we found that NH_3 treatment improved the ORR activity of Co-PDAP (Figure S2). NH_3-treated Co-PDAP has a large Brunauer−Emmett−Teller (BET) surface area (568 m² g⁻¹, measured using powders not loaded on an electrode) as described elsewhere,[11] which may be related to its high ORR activity. The M-PDAP catalysts used here were pyrolyzed in the presence of NH_3 unless otherwise specified.

To evaluate self-supporting Co-PDAP, three types of known Co-coordinating electrode catalysts, namely, Co-polypyrrole/C (Co-PPY/C),[8c] Co-PANI/C,[8d] and cobalt(II) tetrakis(*meso*-4-methoxyphenyl)porphyrin (Co-TMPP/C),[12] were also synthesized, and their ORR activities were compared using a rotating ring disc electrode (RRDE) system at a catalyst loading of 1 mg cm⁻² in phosphate buffer solution (PBS) at pH 7. Steady-state disk currents in the RRDE tests indicated that the Co-PDAP catalyst had the highest ORR activity among the four in terms of onset potential and oxygen-diffusion-limited current density (Figure S3 and Table S2). The ORR onset potential of the Co-PDAP catalyst was 0.82 ± 0.01 V vs reversible hydrogen electrode (RHE) [mean ± standard deviation (SD), n = 3] in PBS, which was the most positive among the values for the four catalysts. The steady-state diffusion current density of Co-PDAP was ~6 mA cm⁻², which was higher than those of the other catalysts. The high limiting current density of Co-PDAP may be due to efficient O_2 diffusion into the porous Co-PDAP catalysts, and the high ORR onset potential of Co-PDAP is likely due to the high density of ORR catalytic centers (Co) in the Co-PDAP catalyst. These ideas are based on the results of the BET (Figure S4) and X-ray photoelectron spectroscopy (XPS) (Figure S5 and Table S3) analyses of the four catalysts.

According to a previous study,[13] we also examined the metal species coordinated to PDAP and found that binary coordination of Co and Fe (CoFe-PDAP) performed better than single coordination of Co or Fe (Figure S6), possibly because of the increase in coordinated metal species (Table S4). The ORR activity of CoFe-PDAP (pyrolyzed at 700 °C in the presence of

NH_3) in the RRDE system in PBS was also compared with that of a Pt/C reference catalyst. These catalysts were loaded on disk electrodes at the same density (0.5 mg$_{total}$ cm⁻²) using Nafion as a binder, and their ORR activities were measured at a rotation speed of 1500 rpm and a scan rate of 5 mV s⁻¹. presents Disk current densities over the potential range from 1.1 to 0.1 V vs RHE at pH 7 (Figure 2a) showed that the onset potential for the
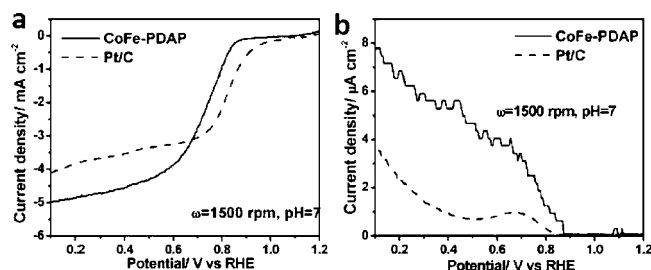

Figure 2. RRDE (a) disk and (b) ring currents showing the ORR activities of CoFe-PDAP and Pt/C (0.5 mg$_{total}$ cm⁻¹ loading) in PBS.

ORR activity of CoFe-PDAP (0.87 ± 0.01 V vs RHE; also deduced from the Tafel plot in Figure S7) was ~0.08 V lower than that of Pt/C (0.95 V ± 0.01 V vs RHE). The half-wave potentials for CoFe-PDAP and Pt/C estimated from the RRDE plots were 0.76 ± 0.02 and 0.84 ± 0.01 V vs RHE, respectively. Also the limiting current density of CoFe-PDAP was 4.9 ± 0.2 mA cm⁻² at 0.2 V, which is substantially higher than that of Pt/C (3.8 ± 0.2 mA cm⁻² at 0.2 V). The onset potential of CoFe-PDAP is substantially higher than those of previously reported NPMCs in neutral PBS (e.g., 0.82 V vs RHE for Fe/Fe₃C−C[2a] and 0.52 V vs RHE for N-doped graphene).[9d] In a solution of H_2SO_4 (pH 2), it was found that the ORR onset and half-wave potentials of CoFe-PDAP (0.84 and 0.73 V vs RHE, respectively) were ~0.1 V lower than those of Pt/C (0.93 and 0.83 V vs RHE, respectively) (Figure S8); these values are comparable to those for active ORR catalysts reported previously.[8d]

The ORR occurs by either two-electron (2e) reduction (to form peroxide species) or four-electron (4e) reduction (to form H_2O). To verify the type of ORR catalyzed by CoFe-PDAP, amperometric responses of the Pt ring electrodes in the RRDE system were also monitored to detect peroxide species formed at the disc electrode[14] (Figure 2b). The number of electrons transferred per O_2 (n) in the ORR at the disc electrode was calculated using the equation $n = 4I_D/(I_D + I_R/N)$, where I_D and I_R are the kinetic currents from the disk and ring electrodes, respectively, and N is the collection efficiency of hydroperoxide (0.19).[9d] From the data in Figure 2, n = 3.96 for CoFe-PDAP at pH 7; this is slightly lower than for Pt/C (n = 3.99). These values indicate that the ORR catalyzed by CoFe-PDAP is mainly the 4e reduction.

Scanning electron microscopy (SEM) images of self-supporting PADP catalysts (either pyrolyzed or not, and treated with NH_3 or not) showed that the surface morphology was changed by pyrolysis (Figure 3). After pyrolysis, although the particle sizes were not changed, the surface became rough, and nanosized pores formed (Figure 3d). In addition, surface pores and cracks were found to be more abundant upon pyrolysis in the presence of NH_3 (Figure 3f). Energy-dispersive spectroscopy (EDS) combined with SEM (EDS-SEM) was used to confirm the elemental distribution in the CoFe-PDAP sample (Figure S9). Uniform distributions of Fe, Co, and N in CoFe-PDAP were detected by recording the X-ray map in the EDS-SEM analysis.
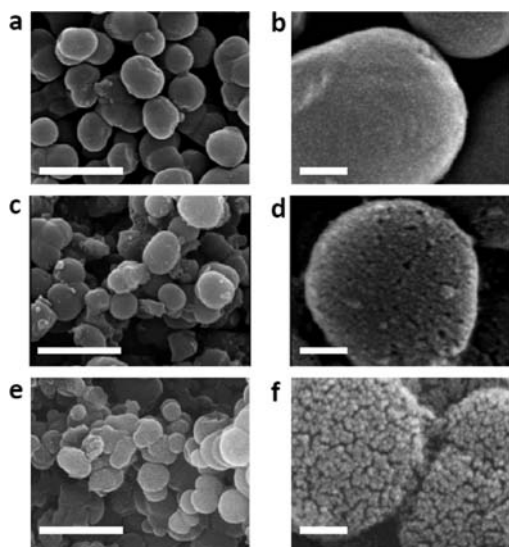
Figure 3. SEM images of (a, b) PDAP before pyrolysis and (c, d) CoFe-PDAP after pyrolysis in the absence of NH_3 and (e, f) CoFe-PDAP after pyrolysis in the presence of NH_3, showing particle sizes and surface morphologies. Scale bars: (a, c, e) 1 μm; (b, d, f) 100 nm.

The C, N, O, Co, and Fe contents determined by the EDS-SEM mapping were 81.5, 9.7, 6.87, 0.52, and 1.43%, respectively. The BET surface area of the pyrolyzed CoFe-PDAP powder sample was 635 m^2 g^{-1}, which is substantially higher than that of Co-PDAP. N_2 absorption/desorption analyses revealed typical type-IV isotherms (as defined by IUPAC[15]), indicating that the CoFe-PDAP catalyst contained a large number of macropores in addition to mesopores centered at ~4 nm in diameter (Figure S10). It is likely that the meso- and macropores resulted in the large surface area and high limiting current densities. On the basis of XPS analyses[16] (Figure S11), the atomic composition in CoFe-PDAP was determined to be 88.7% C, 9.5% N, 0.6% O, 0.3% Co, and 0.9% Fe. The Fe and Co contents determined by XPS are lower than those obtained from the EDS-SEM mapping, probably because of enrichment of these metals close to the surface. A prominent feature is the high surface N content relative to previously reported polymer-type NPMCs such as CoFe-PANI/C (4% as determined by XPS[2b]). It is also important to identify the forms of nitrogen to deduce whether these N atoms can serve as metal-coordination sites. In the XPS analysis (Figure S11), the N 1s spectra were deconvoluted into four peaks (pyridinic N, pyrrolic N, quaternary N, and pyridinic N^+-O^-) according to binding energies;[17] from this analysis, these four types of N atoms were estimated to represent 54, 6, 37, and 3%, respectively, of the total N in CoFe-PDAP. Among them, pyridinic and pyrrolic species are found at the edge of graphitic structures. Because of their electron-donating properties, appropriately arranged pyridinic N atoms can serve as metal-coordination sites. Furthermore, protons and O_2 molecules are trapped by free pyridinic N and subsequently transferred to catalytic sites in ORR catalysts. It is therefore likely that the high contents of pyridinic N and transition metals in CoFe-PDAP are responsible for its high ORR activity. The Fe 2p and Co 2p XPS spectra of CoFe-PDAP sample were also deconvoluted (Figsure S11). Multiple peaks of deconvoluted Fe 2p and Co 2p XPS spectra indicated that metal species in the catalysts were complicated in terms of their metallic state. According to a previous report,[18] the Fe 2p and Co 2p peaks at 711.3 and 781.8

eV, respectively, are due to the N-coordinated metals, which are the dominant metal species in CoFe-PDAP.

Two different models have been proposed to explain active sites in M/C/N catalysts for the ORR, including (1) N-binding metal species[19] and (2) N atoms of CN_x.[20] For CN_x catalysts without metals, the active sites are considered to be related to electron-rich N atoms having electron lone pairs and electron-donating conjugated π-bond systems. On the other hand, the ORR activity of CoFe-PDAP is possibly due to the first model for the following reasons. First, the onset and half-wave potentials of Co-PDAP were strongly influenced by the concentration of bound metals (Tables S1, S3, and S4 and Figures S1, S3, and S6). Second, the ORR activity of pyrolyzed pure PDAP catalyst was greatly improved after the introduction of Co and/or Fe (Figure S6 and Table S4). Although further experiments (e.g., X-ray absorption fine-structure analyses to identify the fine structures of metal-binding sites) are necessary to confirm this idea, our finding that the abundance of the Fe$-N_x$ and Co$-N_x$ structures strongly influences the ORR activity suggests the importance of these structures for the ORR activity of CoFe-PDAP.

Although some NPMCs exhibit relatively high ORR activities, their stabilities are of prominent concern.[21] To evaluate the stability of CoFe-PDAP for ORR, continuous cyclic voltammetry (CV) and RRDE tests were performed in O_2-saturated solutions (Figure S12). In CV, a characteristic reduction current with a well-defined cathodic peak at +0.6 V vs RHE was observed for the CoFe-PDAP electrode in an O_2-supplied electrolyte. In the CV test, the ORR activity was unchanged over 14 days of continuous operation. No obvious decrease in the current density or shift in the ORR potential was observed during the experiment, demonstrating the high stability of CoFe-PDAP in acidic media. In the RRDE test, the ORR catalytic current of CoFe-PDAP in the 3000th sweep was almost the same as that in the first sweep, also proving the high stability of CoFe-PDAP. Comparison of the XPS spectra of the elements in the CoFe-PDAP catalysts before and after the CV stability test (Figure S13) showed that there was no change in elemental composition, demonstrating that Co and Fe are stably coordinated to PDAP. We next examined the effect of methanol on the ORR activity of CoFe-PDAP to check crossover effects of organics. We performed RRDE tests in the presence and absence of methanol (Figure S14) and found that although it had a serious influence on the ORR activity of Pt/C, no effect was observed for CoFe-PDAP. These results demonstrate the promising features of CoFe-PDAP as a stable ORR catalyst in fuel cells.

To evaluate the utility of CoFe-PDAP as a cathode catalyst in MFCs, single-chamber MFCs, each equipped with a carbon-felt anode (4 cm^2 in projection area) and a membrane-type air cathode (1 cm^2) coated with a cathode catalyst (either CoFe-PDAP or Pt/C loaded at 4 mg cm^{-2}), were constructed. Operation was initiated by inoculating the MFCs with rice paddy soil and supplying them with a mixture of starch, peptone, and fish extract, and their electric outputs were monitored using a voltage logger. After the cell voltages became stable, these MFCs were subjected to polarization analyses[2c,22] (Figure 4). From repeated operation of the MFCs ($n = 5$), the short-circuit current density, open-circuit voltage, and maximum power density for MFCs equipped with the CoFe-PDAP cathode were determined to be 0.53 ± 0.05 mA cm^{-2}, 0.7 ± 0.01 V, and 0.11 ± 0.01 mW cm^{-2}, respectively, while those for the Pt/C MFCs were 0.18 ± 0.02 mA cm^{-2}, 0.6 ± 0.02 V, and 0.05 ± 0.005 mW cm^{-2}, respectively (all values mean ± SD). Anode and cathode polarization analyses (Figure S15) revealed that not only the

19530

dx.doi.org/10.1021/ja3085934 | *J. Am. Chem. Soc.* 2012, 134, 19528–19531
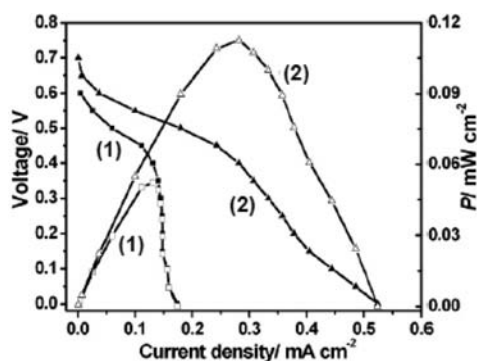
Figure 4. Representative polarization (closed symbols) and power density (open symbols) curves for MFCs equipped with the (1) Pt/C or (2) CoFe-PDAP cathode catalyst loaded at 4 mg cm^{-2}.

cathode but also the anode of the CoFe-PDAP MFCs showed higher performance than those in the Pt/C MFCs. The superior activity of the CoFe-PDAP cathode is due to the lessened crossover effects of organics on the ORR activity of CoFe- compared with Pt/C. The reasons for the higher anode performance in the CoFe-PDAP MFCs are not clear, but the loss of organics-oxidation activity at the cathode may have positively affected the anode performance. The performance of the CoFe-PDAP MFCs was stable during continuous operation for 1 month, while that of the Pt/C MFCs gradually decreased during the same period (Figure S16). These results indicate the promising features of CoFe-PDAP as a cathode catalyst in MFCs.

The present study shows a design concept for synthesizing polymer-derived ORR catalysts. We successfully synthesized the self-supporting M-PDAP catalysts using cheap raw materials (DAP, Co, and Fe). The M-PDAP catalysts developed in this work exhibited high ORR onset and half-wave potentials, suggesting their utility as efficient cathode catalysts for energy-conversion devices, including MFCs. Since a huge repertoire of N-containing aromatic compounds is present in databases, we expect that excellent building-block monomers exist among them. These compounds must be screened for the synthesis of highly active NPMCs for the ORR. In addition, a better understanding of the reaction mechanism of the CoFe-PDAP catalyst must be obtained to provide insights into new design concepts for active and stable ORR catalysts.

■ ASSOCIATED CONTENT

Ⓢ Supporting Information

Experimental section and additional data. This material is available free of charge via the Internet at http://pubs.acs.org.

■ AUTHOR INFORMATION

Corresponding Author
kazuyaw@toyaku.ac.jp; hashimoto@light.t.u-tokyo.ac.jp

Notes

The authors declare no competing financial interest.

■ ACKNOWLEDGMENTS

■ REFERENCES

(1) Zhang, G. Q.; Zhang, X. G.; Wang, Y. G. *Carbon* **2004**, *42*, 3097.

(2) (a) Wen, Z. H.; Ci, S. Q.; Zhang, F.; Feng, X. L.; Cui, S. M.; Mao, S.; Luo, S. L.; He, Z.; Chen, J. H. *Adv. Mater.* **2012**, *24*, 1399. (b) Jaouen, F.; Proietti, E.; Lefèvre, M.; Chenitz, R.; Dodelet, J. P.; Wu, G.; Chung, H. T.; Johnson, C. M.; Zelenay, P. *Energy Environ. Sci.* **2011**, *4*, 114. (c) Watanabe, K. *J. Biosci. Bioeng.* **2008**, *106*, 528.

(3) (a) Berger, D. J. *Science* **1999**, *286*, 49. (b) Rozendal, R. A.; Hamelers, H. V.; Rabaey, K.; Keller, J.; Buisman, C. J. *Trends Biotechnol.* **2008**, *26*, 450.

(4) Bezerra, C. W. B.; Zhang, L.; Lee, K. C.; Liu, H. S.; Marques, A. L. B.; Marques, E. P.; Wang, H. J.; Zhang, J. J. *Electrochim. Acta* **2008**, *53*, 4937.

(5) Jasinski, R. *Nature* **1964**, *201*, 1212.

(6) (a) Ziegelbauer, J. M.; Olson, T. S.; Pylypenko, S.; Alamgir, F.; Jaye, C.; Atanassov, P.; Mukerjee, S. *J. Phys. Chem. C* **2008**, *112*, 8839. (b) Li, W.; Yu, A.; Higgins, D. C.; Llanos, B. G.; Chen, Z. *J. Am. Chem. Soc.* **2010**, *132*, 17056.

(7) (a) Qu, L. T.; Liu, Y.; Baek, J. B.; Dai, L. M. *ACS Nano* **2010**, *4*, 1321. (b) Wang, P.; Wang, Z.; Jia, L.; Xiao, Z. *Phys. Chem. Chem. Phys.* **2009**, *11*, 2730.

(8) (a) Gupta, S.; Tryk, D.; Bae, I.; Aldred, W.; Yeager, E. *J. Appl. Electrochem.* **1989**, *19*, 19. (b) Bashyam, R.; Zelenay, P. *Nature* **2006**, *443*, 63. (c) Yuan, X.; Zeng, X.; Zhang, H. J.; Ma, Z.-F.; Wang, C. Y. *J. Am. Chem. Soc.* **2010**, *132*, 1754. (d) Wu, G.; More, K. L.; Johnston, C. M.; Zelenay, P. *Science* **2011**, *332*, 443.

(9) (a) Zhao, F.; Harnisch, F.; Schröder, U.; Scholz, F.; Bogdanoff, P.; Herrmann, I. *Environ. Sci. Technol.* **2006**, *40*, 5193. (b) Ahmed, J.; Yuan, Y.; Zhou, L. H.; Kim, S. *J. Power Sources* **2012**, *208*, 170. (c) Chen, S. L.; Chen, Y.; He, G. H.; He, S. J.; Schröder, U.; Hou, H. Q. *Biosens. Bioelectron.* **2012**, *34*, 282. (d) Feng, L. Y.; Chen, Y. G.; Chen, L. *ACS Nano* **2011**, *5*, 9611. (e) Yuan, Y.; Zhao, B.; Jeon, Y.; Zhong, S. K.; Zhou, S. G.; Kim, S. *Bioresour. Technol.* **2011**, *102*, 5849. (f) Feng, L. Y.; Yan, Y. Y.; Chen, Y. G.; Wang, L. J. *Energy Environ. Sci.* **2011**, *4*, 1892.

(10) Downey, J. S.; Frank, R. S.; Li, W.-H.; Stöver, H. D. H. *Macromolecules* **1999**, *32*, 2838.

(11) Meng, M.; Larouche, N.; Lefèvre, M.; Jaouen, F.; Stansfield, B.; Dodelet, J. P. *Electrochim. Acta* **2010**, *55*, 6450.

(12) Zhang, W.; Shaikh, A. U.; Tsui, E. Y.; Swager, T. M. *Chem. Mater.* **2009**, *21*, 3234.

(13) Lefèvre, M.; Proietti, E.; Jaouen, F.; Dodelet, J. P. *Science* **2009**, *324*, 71.

(14) Paulus, U. A.; Schmidt, T. J.; Gasteiger, H. A.; Behm, R. J. *J. Electroanal. Chem.* **2001**, *495*, 134.

(15) Sing, K. S. W.; Everett, D. H.; Haul, R. A. W.; Moscou, L.; Pierotti, R. A.; Rouquerol, J.; Siemieniewska, T. *Pure Appl. Chem.* **1985**, *57*, 603.

(16) Beamson, G.; Briggs, D. *High-Resolution XPS of Organic Polymers: The Scienta ESCA A300 Database*; Wiley: Chichester, U.K., 1992.

(17) Kelemen, S. R.; Afeworki, M.; Gorbaty, M. L.; Kwiatek, P. J. *Energy Fuels* **2002**, *16*, 1507.

(18) Wu, G.; Chen, Z. W.; Artyushkova, K.; Garzon, F. H.; Zelenay, P. *ECS Trans.* **2008**, *16*, 159.

(19) (a) Faubert, G.; Lalande, G.; Cote, R.; Guay, D.; Dodelet, J. P.; Weng, L. T.; Bertrand, P.; Denes, G. *Electrochim. Acta* **1996**, *41*, 1689. (b) Lefevre, M.; Dodelet, J. P.; Bertrand, P. *J. Phys. Chem. B* **2002**, *106*, 8705.

(20) (a) Nabae, Y.; Moriya, S.; Matsubayashi, K.; Lyth, S. M.; Malon, M.; Wu, L.; Islam, N. M.; Koshigoe, Y.; Kuroki, S.; Kakimoto, M.-a.; Miyata, S.; Ozaki, J.-i. *Carbon* **2010**, *48*, 2613. (b) Ikeda, T.; Boero, M.; Huang, S.-F.; Terakura, K.; Oshima, M.; Ozaki, J.-i. *J. Phys. Chem. C* **2008**, *112*, 14706.

(21) Gong, K.; Du, F.; Xia, Z.; Dustock, M.; Dai, M. *Science* **2009**, *323*, 760.

(22) Zhao, Y.; Watanabe, K.; Nakamura, R.; Mori, S.; Liu, H.; Ishii, K.; Hashimoto, K. *Chem.—Eur. J.* **2010**, *16*, 4982.